Synthesis and Field Emission Characteristics of Bilayered ZnO Nanorod Array Prepared by Chemical Reaction

Hui Zhang, Deren Yang,* Xiangyang Ma, and Duanlin Que

State Key Laboratory of Silicon Materials, Zhejiang University, Hangzhou 310027, People's Republic of China

Received: March 8, 2005; In Final Form: July 7, 2005

The uniform, large-scale, and bilayered ZnO nanorod array on silicon substrate has been synthesized by a catalyst and template-free chemical reaction in a dilute solution. The effect of different precursor ZnO films on the morphology and size of the ZnO nanorod array has been investigated. Moreover, the morphology evolution of the ZnO nanorod array with the increase of reaction time indicates that the second growth is the reason for the decrease of the ZnO nanorod diameter and the formation of the bilayered ZnO nanorod array. Finally, the field emission from the ZnO nanorod array with different diameters is presented.

Introduction

In recent years, the research interests on the quasi one-dimensional semiconductors have been greatly spurred due to their essential scientific and technological significance.[1] While the synthesis of arrayed one-dimensional nanostructures seems more important for the fabrication of field emission and other devices. In the past decade, carbon-based materials such as diamond, diamond-like carbon, carbon nanotube, and amorphous carbon have been the main candidates for the field emission due to their low work function, high mechanical stability, high aspect ratio, and high conductivity.[2] As an important semiconductor, ZnO, with a wide band gap (3.2 eV) and large exciton binding energy of 60 meV at room temperature, has attracted considerable attention and is of interest for low-voltage and short-wavelength electrooptical nanodevices. Moreover, ZnO one-dimensional array has become a good candidate for field emission because of their thermal stability, oxide resistibility, and high aspect ratio, which spurs the research on the synthesis of the ZnO one-dimensional array.[3] However, the previous report on the synthesis of the ZnO one-dimensional array mostly focused on the vapor-phase processes such as thermal evaporation, chemical vapor deposition, and so on.[4] Recently, Vayssieres et al. has reported a simple solution approach to synthesis of the ZnO nanorod and microtube arrays by low-temperature hydrothermal process on silicon substrate.[5] In particular, the synthesis of wafer-scale ZnO nanorod arrays by direct chemical reaction on silicon substrate provides a low-cost, simple, large-scale, practical method. The idea for the synthesis of the ZnO nanorod array by chemical reaction is based on a two-step process including the deposition of a crystal seed layer on the substrate and subsequent aqueous chemical growth.[6] However, compared with the vapor-phase process, the problem of uneven and large diameter of ZnO nanorod array derived by chemical reaction should be solved. Herein, we report the synthesis of bilayered ZnO nanorod array by a catalyst and template-free chemical reaction in a dilute solution, in which the second growth mechanism for the decrease of the ZnO nanorod array diameter and the formation of a bilayered ZnO nanorod array, which is in line with the previously reported concentration dependency of the nanorod diameter by Vayssieres et al.[5] Moreover, the effects of different precursor ZnO films on the morphology and size of the ZnO nanorod array are investigated. Finally, the field emission from the bilayered ZnO nanorod array is presented.

* To whom correspondence should be addressed. E-mail: mseyang@zju.edu.cn.

Experimental Section

Two kinds of precursor ZnO film as the seed layers were synthesized by spin coating and sputtering on silicon substrate, the detailed experimental conditions of which can be found in previous references.[6a,7] For the fabrication of ZnO nanorod array, the following experiments were performed: 890 mg of $Zn(NO_3)_2$ and 420 mg of diethylenetriamine were respectively dissolved into 100 mL of deionized water. After 10 min of stirring, the two solutions were mixed. Subsequently, the mixed solution was kept at 90 °C. And then, the silicon substrates were hung vertically to the bottom of the beaker in the mixed solution for different times of 1, 2, and 3 h. After the reaction was complete, the substrates were then removed from the solution, rinsed in deionized water, and then dried.

The obtained samples were characterized by X-ray powder diffraction (XRD) using a Japan Rigaku D/max-ga X-ray diffractometer with graphite monochromatized Cu Kα radiation ($\lambda = 1.541\,78$ Å). The field emission scan electron microscope (FESEM) images were obtained on FEI SIRION.

Results and Discussion

Figure 1 shows the FESEM images of two samples prepared by the chemical reaction for 3 h on silicon substrate with a precursor ZnO film prepared by spin coating or sputtering. As shown in Figure 1a,b, on the silicon substrate with the precursor ZnO film prepared by spin coating, the disordered flowerlike ZnO nanostructures consisting of nanorods with diameters of more than 100 nm are observed. While on the silicon substrate with the precursor ZnO film prepared by sputtering, large-scale, uniform, and vertically arrayed ZnO nanorods with diameters of about 30 nm were formed, as shown in Figure 1c,d. The above results indicate that the precursor ZnO films dictated the morphology and size of the ZnO nanorods formed in the subsequent chemical reaction. As we know, the growth of the arrayed ZnO nanorods initiating from the precursor ZnO film

10.1021/jp051204a CCC: $30.25
Published on Web 08/18/2005

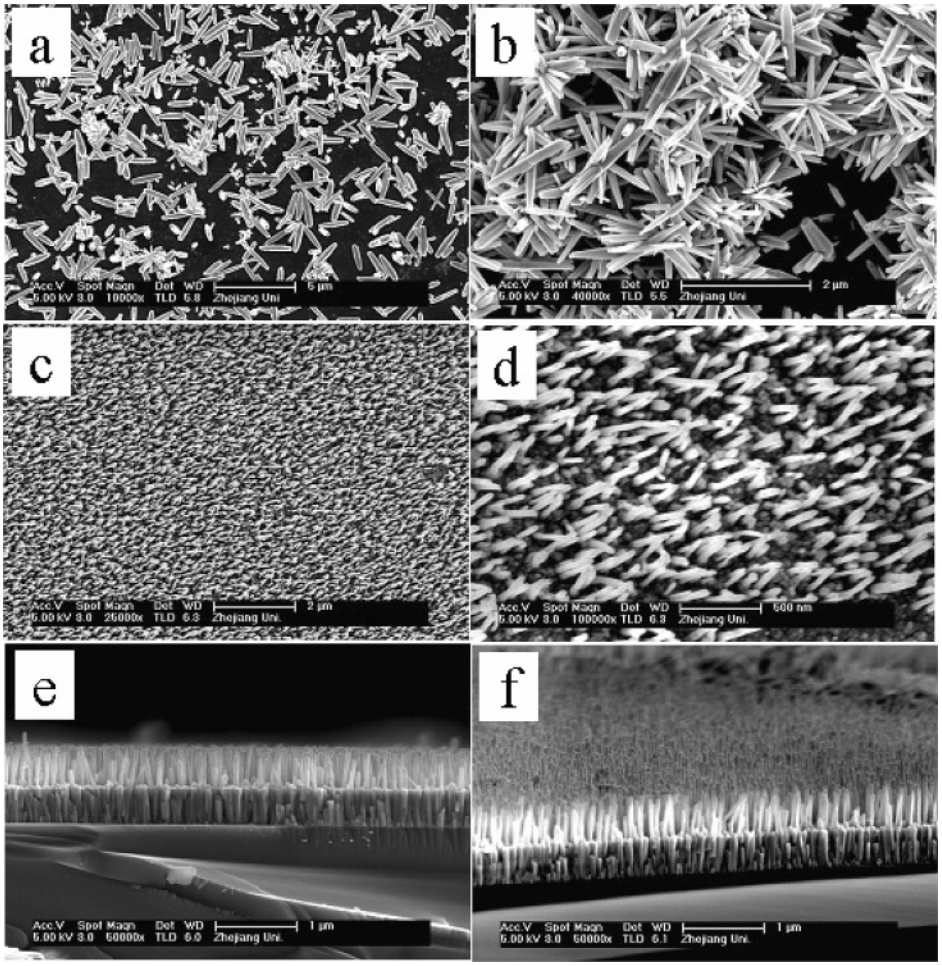

Figure 1. FESEM images of ZnO nanostructures prepared by chemical reaction in a dilute solution for 3 h on different precursor ZnO films synthesized by (a, b) spin coating and (c, d) sputtering. Cross-sectional FESEM images of the sample corresponding to images c and d are shown in e and f.

during the chemical reaction process is controlled by epitaxial growth mechanism, which has been reported previously in ref 8. Therefore, the higher preferential orientation of ZnO precursor film prepared by sputtering facilitated the vertical growth of ZnO nanorods. The cross-sectional FESEM observation of the arrayed ZnO nanorods revealed that the ZnO array was actually composed of two layers of ZnO nanorods with different lateral sizes as shown in Figure 1e,f. Compared with the previous report where single-layered ZnO nanorod array was achieved in a concentrated solution by chemical reaction on a spin-coated ZnO precursor film,[6a] herein, the bilayered ZnO nanorod array was derived from a dilute solution on a sputtered ZnO precursor film, the reason for which will be discussed later.

Figure 2 shows the XRD patterns of the above-mentioned two samples. All the diffraction peaks in the two patterns can be indexed as the hexagonal ZnO, according to the standard card (JCPDS 36-1451). The much larger ratio between the (002) and other low-intensity peaks in the XRD pattern of arrayed ZnO nanorods compared with that of flowerlike ZnO nanostructures indicates that the arrayed ZnO nanorods are aligned well vertically almost along the [001] direction, which is in accordance with the results of FESEM.

To clarify the underlying growth mechanism for the bilayered ZnO nanorod array formed by the chemical reaction, Figure 3 shows scenario images for the morphology evolution from the precursor ZnO film to the bilayered ZnO nanorod array. The morphology of the sputtered ZnO film is shown in Figure 3a, as can be seen, the film's grain sizes range in 100−300 nm.

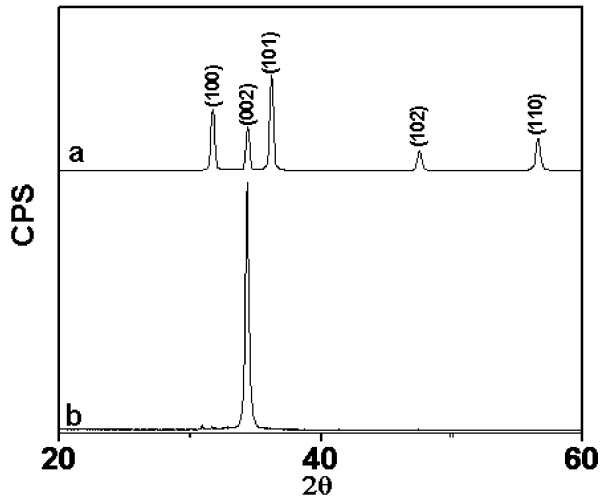

Figure 2. XRD patterns of ZnO nanostructures prepared by chemical reaction in a dilute solution for 3 h on the different precursor ZnO films synthesized by (a) spin coating and (b) sputtering.

After 1 h chemical reaction, the ZnO nanorods began to vertically grow initiating from the grains of the precursor film, as shown in Figure 3b. A black dot on the top of each ZnO nanorod can be observed from the magnified image inserted in Figure 3b, indicating that the top of the ZnO nanorod is hollow. Therefore, it is believed that the ZnO nanorods initially formed on the grain of the precursor film by epitaxial growth mechanism, and the lateral growth was from outside to inside. With

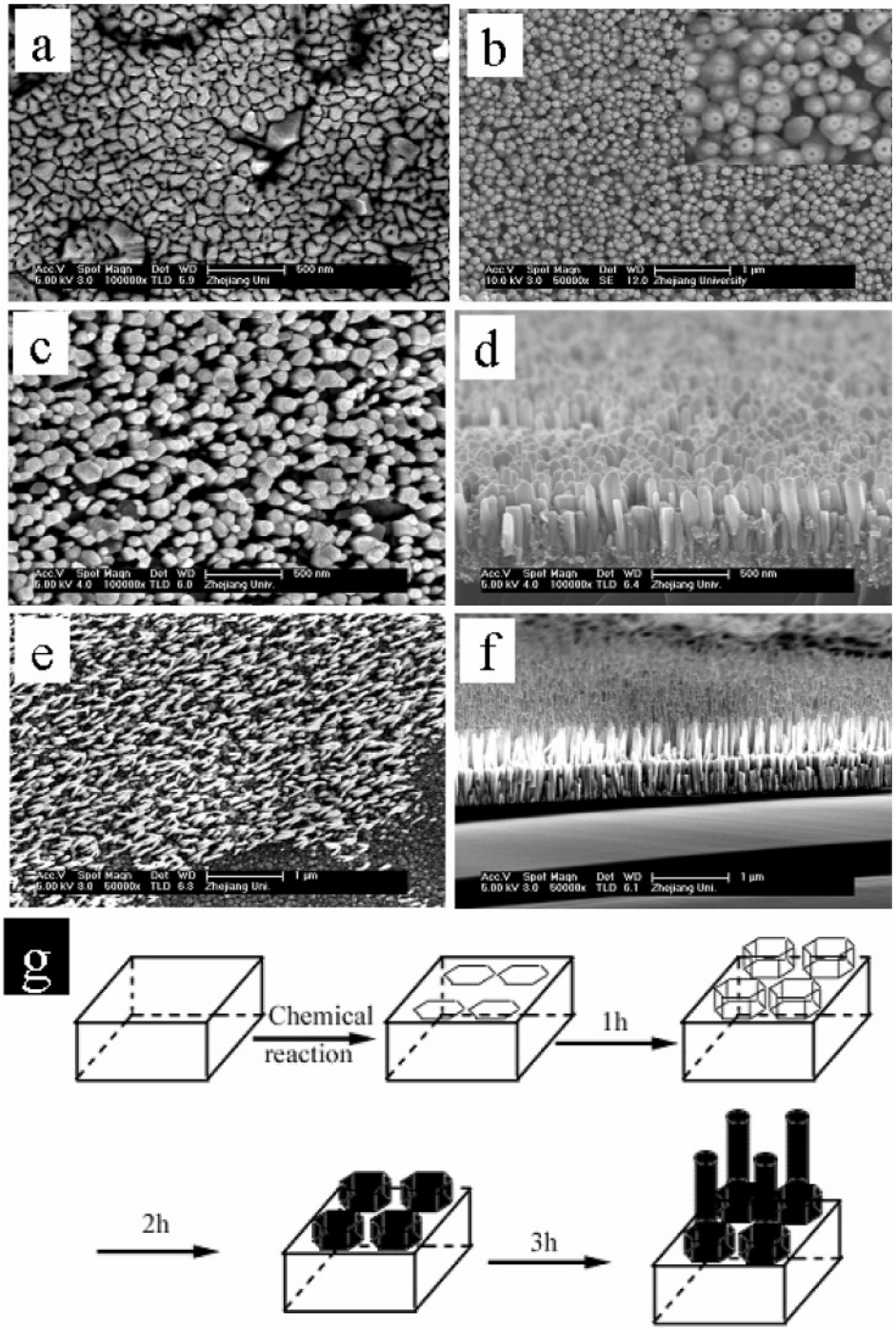

Figure 3. FESEM images of ZnO nanostructures prepared by chemical reaction in a dilute solution on the precursor ZnO films sputtered for different times: (a) 0, (b) 1, (c, d) 2, and (e, f) 3 h. (g) The schematic sketch of the morphology evolution of the arrayed ZnO nanorod with the increase of reaction time.

the extension of the chemical reaction, as shown in Figure 3c,d, the bottom layer of the ZnO nanorod arrays had already been formed and the secondary growth of ZnO nanorods was initiated from the bottom layer. Finally, as the chemical reaction proceeded long enough (about 3 h), the top layer of the ZnO nanorods with a smaller diameter of about 30 nm was formed on the bottom layer of the ZnO nanorod, as shown in Figure 3e,f. The morphology evolution of the ZnO nanorod array with increasing reaction time can be summarized by the diagrammatic sketch shown in Figure 3g. At the early stage of the chemical reaction, the hexagonal prisms of ZnO were first formed on the precursor ZnO film, growing transversely from the periphery to the center. With the extension of the reaction, due to the ever-decreasing solution concentration, the transversal growth became increasingly slow so that the growth of ZnO nanorods could not proceed with the original diameters. Instead, the second growth of ZnO nanorods with smaller diameter occurred, ultimately resulting in the bilayered ZnO nanorod array. It should be mentioned that in the second growth of ZnO nanorods the diameter was almost determined by the concentration of solution. Therefore, the top-layer ZnO nanorods were quite uniform with smaller diameter. Moreover, the reason for the formation of the ZnO nanorods with the cusp end was presented by our previous reports.[9]

The field emission from the bilayered ZnO nanorod arrays was measured in a vacuum chamber at a pressure of 1×10^{-6}

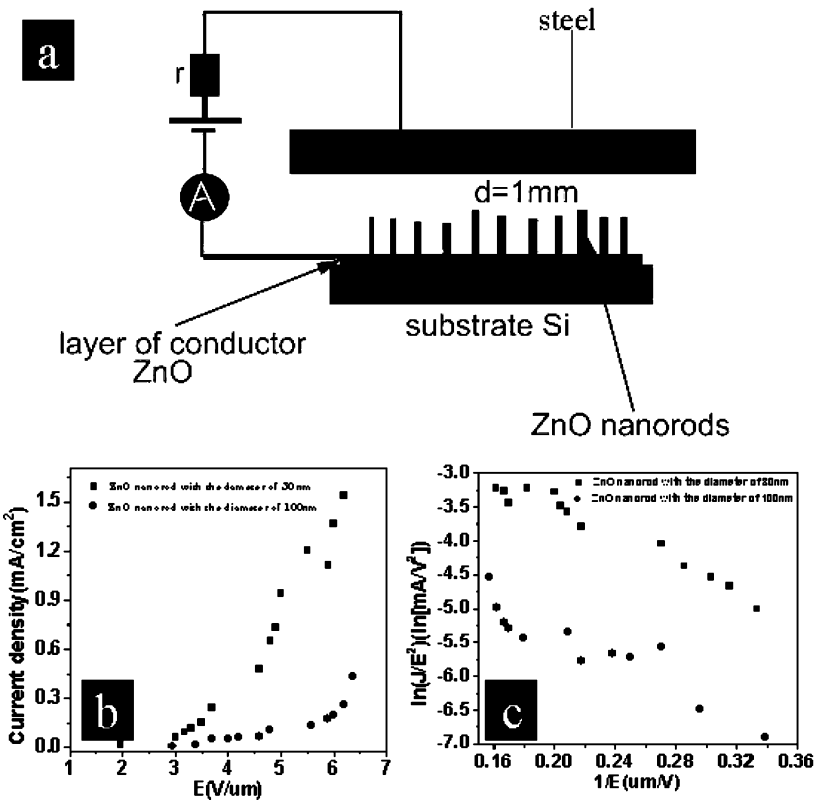

Figure 4. Schematic sketch of the measurement for field emission (a); the field emission current density as a function of the applied electric field of the ZnO nanorod array with different diameters (b); the FN plot of field emission current density vs electric field for the ZnO nanorod array with different diameters (c).

Pa at room temperature. The ZnO array on the silicon substrate was attached to a stainless steel plate as the cathode in the face of the other stainless steel plate as the anode, as shown in Figure 4a. Figure 4b illustrates the emission current density as a function of the applied field for the bi-layered ZnO nanorod arrays with different diameters. As extrapolated from Figure 4b, with the decrease of the ZnO nanorod diameter, the turn-on electric field at a current density of 0.1 mA/cm^2 and the threshold field at a current density of 1 mA/cm^2 decreased, indicative of the better field emission characteristics of the ZnO nanorods with diameters of 30 nm. Moreover, the turn-on and threshold electric fields of ZnO nanorods with diameters of 30 nm are equal to 2 and 5 V/μm, respectively, which is comparable to the recently reported data of carbon-based materials and ZnO nanomaterials.[10] It is believed that the existence of sharp tips in the ZnO nanorods contributed to the desirable field emission performance.

The field emission characteristics are also evaluated by the simplified Fowler−Nordheim (FN) equation:

$$J = (A\beta^2E^2/\phi)\exp(-B\phi^{3/2}\beta E) \quad (1)$$

where β is the field enhancement factor, φ is the work function of the electron emitter, A and B are the constants with values of 1.56×10^{-10} (A V^{-2} eV) and 6.83×10^9 (V eV$^{-3/2}$ μm^{-1}), respectively. Figure 4c shows the experimental data of $\ln(J/E^2)$ as a function of $1/E$ for the ZnO nanorod arrays with diameters of 30 and 100 nm, respectively. The nearly linear relationship between $\ln(J/E^2)$ and $1/E$ for the ZnO array with different diameters can be derived, indicating that the emission is attributed to the field emission. Using the reported work function of ZnO (5.3 eV), the estimated field enhancement factor β of the ZnO array with a diameter of 30 nm is equal to 1680, which is larger than that of the ZnO array with a diameter of 100 nm. Therefore, it is clear that reducing the diameter of the ZnO nanorod is critical for improving the field emission characteristics.

Conclusions

In summary, the uniform, large-scale, and bilayered ZnO nanorod array on the silicon substrate has been prepared by a catalyst and template-free chemical reaction in a dilute solution. It is found that the second growth induced by the dilute solution is the main reason for the diameter decrease and the formation of bilayered ZnO nanorod array. The ZnO nanorod array with smaller diameter shows the better field emission performance. It is anticipated that the method presented in this work offers a solution to forming the bilayered structure of nanomaterials.

Acknowledgment. The authors appreciate the financial support from the Natural Science Foundation of China (Grant 60225010), the Key Project of the Chinese Ministry of Education, and the Program for New Century Excellent Talents in Universities. Prof. Youwen Wang is thanked for the FESEM measurements.

References and Notes

(1) (a) Duan, X.; Huang, Y.; Agarwal, R.; Lieber, C. M. *Nature* **2003**, *421*, 241. (b) Fuhrer, M. S.; Nygard, J.; Shih, L.; Forero, M.; Yoon, Y. G.; Mazzoni, M. S. C.; Choi, H. J. *Science* **2000**, *288*, 494. (c) Ren, Z. F.; Huang, Z. P.; Xu, J. W.; Wang, J. H.; Bush, P.; Siegal, M. P.; Provencio, P. N. *Science* **1998**, *282*, 1105. (d) Morales, A. M.; Lieber, C. M. *Science* **1998**, *279*, 208. (e) Pan Z. W.; Dai Z. R.; Wang Z. L. *Science* **2001**, *291*, 1947.

(2) (a) Geis, M. W.; Efremow, N. N.; Krohn, K. E.; Twichell, J. C.; Lyszczarz, T. M.; Kalish, R.; Greer, J. A.; Tabat, M. D. *Nature* **1998**, *393*, 431. (b) Kan, M. C.; Huang, J. L.; Sung, J.; Lee, D. F.; Chen, K. H. *J. Am.*

Ceram. Soc. **2003**, *86*, 1513. (c) Fan S. S.; Chapline M. G.; Franklin N. R.; Tombler T. W.; Cassell A. M.; Dai H. J. *Science* **1999**, *283*, 512. (d) Pan, Z. W.; Lai, H. L.; Au, F. C. K.; Duan, X. F.; Zhou, W. Y.; Shi, W. S.; Wang, N.; Lee, C. S.; Wong, N. B.; Lee, S. T.; Xie, S. S. *Adv. Mater.* **2000**, *12*, 1186. (e) Lai, S. H.; Chang, K. L.; Shih, H. C.; Huang, K. P.; Lin, P. *Appl. Phys. Lett.* **2004**, *85*, 6248.

(3) (a) Banerjee, D.; Jo, S. H.; Ren, Z. F. *Adv. Mater.* **2004**, *16*, 2028. (b) Jo, S. H.; Banerjee, D.; Ren, Z. F. *Appl. Phys. Lett.* **2004**, *85*, 1407. (c) Zhu, Y. W.; Zhang, H. Z.; Sun, X. C.; Feng, S. Q.; Xu, J.; Zhao, Q.; Xiang, B.; Wang, R. M.; Yu, D. P. *Appl. Phys. Lett.* **2003**, *83*, 144. (d) Lyu, S. C.; Zhang, Y.; Lee, C. J.; Ruh, H.; Lee, H. J. *Chem. Mater.* **2003**, *15*, 3294.

(4) (a) Hsu, C. L.; Yang, S. S.; Tseng, Y. K.; Chen, I. C.; Lin, Y. R.; Chang, S. J.; Wu S. T. *J. Phys. Chem. B* **2004**, *108*, 18799. (b) Han, X. H.; Wang, G. Z.; Jie, J. S.; Luo, Y.; Yuk, T. I.; Choy, W. C. H.; Hou, J. G. *J. Phys. Chem. B* **2005**, *109*, 2733. (c) Xu, X. Y.; Zhang, H. Z.; Zhao, Q.; Chen, Y. F.; Xu, J.; Yu, D. P. *J. Phys. Chem. B* **2005**, *109*, 1699. (d) Liu, C. H.; Zapien, J. A.; Yao, Y.; Meng, X. M.; Lee, C. S.; Fan, S. S.; Lifshitz, Y.; Lee, S. T. *Adv. Mater.* **2003**, *15*, 838

(5) (a) Vayssieres, L. *Adv. Mater.* **2003**, *15*, 464. (b) Vayssieres, L.; Keis, K.; Lindquist, S. E.; Hagfeldt, A. *J. Phys. Chem. B* **2001**, *105*, 3350. (c) Vayssieres, L.; Keis, K.; Hagfeldt, A.; Lindquist, S. E. *Chem. Mater.* **2001**, *13*, 4395.

(6) (a) Greene, L. E.; Law, M.; Goldberger, J.; Kim, F.; Johnson, J. C.; Zhang, Y.; Saykally, R. J.; Yang, P. D. *Angew. Chem., Int. Ed.* **2003**, *42*, 3031. (b) Yu, H. D.; Zhang, Z. P.; Han, M. Y.; Hao, X. T.; Zhu, F. R. *J. Am. Chem. Soc.*, in press.

(7) Ndong, R.; Ferblantier, G.; Al Kalfioui, M.; Boyer, A.; Foucaran, A. *J. Cryst. Growth* **2003**, *255*, 130.

(8) (a) Park, W. I.; Kim, D. H.; Jung, S. W.; Yi, G. C. *Appl. Phys. Lett.* **2002**, 80, 4232. (b) Renee, B. P.; Clark, L. F.; Brian, A. G. *Langmuir* **2004**, *20*, 5114.

(9) (a) Zhang, H.; Yang, D.; Ma, X.; Ji, Y.; Xu, J.; Que, D. *Nanotechnology* **2004**, *15*, 622. (b) Zhang, H.; Yang, D.; Ji, Y.; Ma, X.; Xu, J.; Que, D. *J. Phys. Chem. B* **2004**, *108*, 3955. (c) Zhang, H.; Yang, D.; Li, D.; Ma, X.; Li, S.; Que, D. *Cryst. Growth Des.* **2005**, *5*, 547.

(10) (a) Wang, M. S.; Peng, L. M.; Wang, J. Y.; Chen, Q. *J. Phys. Chem. B* **2005**, *109*, 110. (b) Jo, S. H.; Lao, J. Y.; Ren, Z. F.; Farrer, R. A.; Baldacchini, T.; Fourkas, J. T. *Appl. Phys. Lett.* **2003**, *83*, 4821. (c) Li, Q. H.; Wan, Q.; Chen, Y. J.; Wang, T. H.; Jia, H. B.; Yu, D. P. *Appl. Phys. Lett.* **2004**, *85*, 634. (d) Dong, L. F.; Jiao, J.; Tuggle, D. W.; Petty, J. M.; Elliff, S. A.; Coulter, M. *Appl. Phys. Lett.* **2003**, *82*, 1096. (e) Lee, C. J.; Lee, T. J.; Lyu, S. C.; Zhang, Y.; Ruh, H.; Lee, H. J. *Appl. Phys. Lett.* **2002**, *81*, 3648. (f) Xu, C. X.; Sun, X. W.; Chen, B. J. *Appl. Phys. Lett.* **2004**, *84*, 1540.